Speed Regulation Enhancement for SRM Drive in PHEV Applications by using Hybrid Fuzzy Logic controller

A.S. Veerendra, M.R. Mohamed, M.H. Sulaiman, K. Peddakapu, K.Sudhakar, Sreenath sukumaran

Abstract: ***Speed regulation enhancement of a Switched Reluctance Motor (SRM) Driveby using modularfront-endintegrated multilevel converter for plug-in hybrid electric vehicle (PHEV) applications are studied and evaluated in this paper. Theoperating modes of the system are basing on Turn-On &Turn OFF of the switches in the converter circuit. In order to achievefast demagnetization and excitation, during generator driving mode, the battery bank is used to elevate the phase voltage. To get the multiple voltage responses and torque increment, an additional charging capacitor and a reframed four-level structure from the converter during battery driving mode is required. A hybrid Fuzzy Logic Controlleris proposedin orderto control the speed of the SRM motor. This paper mainly focuses on the comparison of the hybrid fuzzy logic controller with conventional P & PI and to prove the proposed controller provides the best performance and high robustness compared to a conventional P & PI controller. Matlab / Simulink is used to simulate.***

Keywords: hybrid Fuzzy logic controller, P & PI controller Integrated multi-level converter, electric vehicles (EVs), hybrid EVs (HEVs), switched reluctance motors (SRMs).

I. INTRODUCTION

With continuous effort to reduce the greenhouse gas emission that it is majorly caused due to the Internal combustion engine. To protect the environment, researchers are exploring the alternative fuels. Therefore, electric vehicles (EVs) have involvedcollective attention over the decades[1-4].These electric vehicles run purely with a battery having less pollution, better fuel economy and efficiency Contrasted to conventional internal combustion engine (ICE)-based vehicles. However, the EV has some limitation like high battery weight, short driving range and high charging time. As a result,to compromisepure battery-powered vehicles, Hybrid electric vehicles (HEVs) and plug-in HEVs (PHEVs) are gaininga choice of attraction[5-7].

In HEV and PHEV, motors are playing a prominent role. Among all types of motors permanent-magnet synchronous motors (PMSMs) are majorly using in-vehicle manufacturers due tohigh power density and high-level engine drive technology[8, 9], but the material used in magnets are usually rare earth materials like neodymium (Nd) and dysprosium (Dy).Due to that, PMSM ishaving some limitation such as high cost and high-temperature permanent magnets.Therefore manufacturers exploring a solution for rare-earth-free magnets[10]. Hence to avoid the problems in PMSM, Switched reluctance motors (SRMs) are known to provide longer service time and a more cost-effective option and also works in a harsh environment because of its simpler, more robust design without any permanent rotor windings and magnets gives high efficiency, high reliability, outstanding fault tolerance capability and high starting torque in initial accelerations [11, 12]. From [13], PHEV drivetrain based on SRM comprises of a power control unit that includes an integrated converter and controller,an energy storage unit, an Internal Combustion Engine, and an SRM that operates as a traction motor. The Simulink models are designed separately for PI & hybrid Fuzzy logic controller and are compared with their performance. The Switched Reluctance Motor is an electrical engine running through a torque of reluctance. The controllers used at this time are the conventional PI controller, and the other one is Fuzzy Logic Controller based on Artificial Intelligence. The PI Controller proportional integral controller) is the PID controller's most special case where the error derivative is not used. Hybrid Fuzzy logic haslogical values that resemble human reasoning. HFLC has various applications in industrial control, especially where it is very difficult to apply these conventional control design techniques. A broad review of the modelling, design, simulation and analysis and control of SRM machines [14] has been carried out.

II. CENTRAL-TAPPED WINDINGS SRM TOPOLOGY

Basing on charging methods for PHEV, a split converter methodology is designed for PMSM motors to charge from Grid without basing on charging stations; however, it requires different winding structure and also only suitable for ac charging. Hence an eight pole four phase SRM is proposed in this paper having central-tapped node and half-bridge asymmetric drive topology.To understand front-end modular converter motor drive structure, an

Revised Manuscript Received on July 07, 2019.

A. S. Veerendra, Sustainable Energy & Power Electronics Research (Super) Cluster University Malaysia, Pahang, Malaysia

M.R. Mohamed, Sustainable Energy & Power Electronics Research (Super) Cluster, University Malaysia, Pahang, Malaysia.

K. Sudhakar, Energy Center, MANIT, Bhopal

asymmetric half-bridge converter topology is exploited as revealed in Fig.1.Entailing of Eight metal–oxide–semiconductor field effect transistors (MOSFETs), eight freewheeling diodes, and two inputs filter capacitors ($C_{ab}$and $C_{cd}$are). The winding inductances of phases A, B, C, and D, respectively, are L_{a14}, L_{a23}, L_{b14}, L_{b23}, L_{c14}, L_{c23}, L_{d14}, and L_{d23}. NA, NB, NC, and ND are the four-phase central-tapped nodes. It consisting of two converters such as Converter I drives phases A and B and share the voltage of the E1 battery,while the Converter II drives the C and D phases and share E2. From Figure 1; converters operate in two modes: driving and charging. During driving mode,the converter is equivalent to a conventional half-bridge asymmetric topology, and the charging plug is inactive. Because NA and ND are kept open, seems to be there is no current flowing between NB and NC, i.e. converters I and II operate separately.During Charging modeConverters I and II are in charging state when the charging plug is connected to an external source.

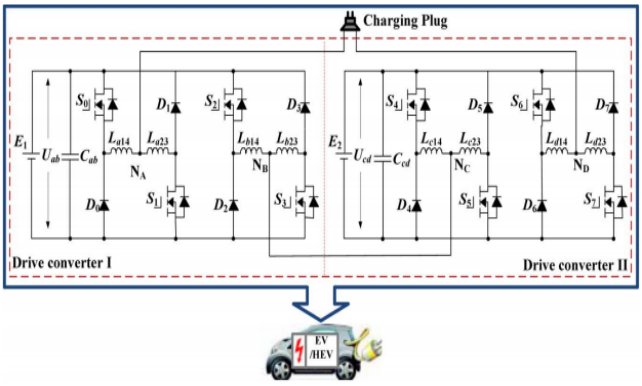

Fig. 1. Central tapped front-end proposed Topology

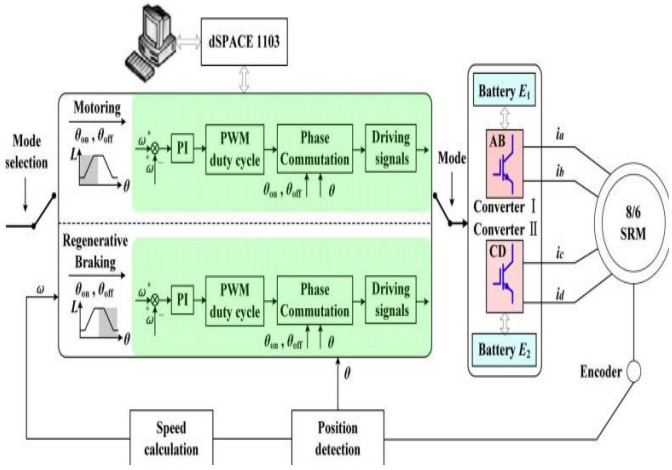

Fig. 2. SRM block diagram control.

III. CONTROL STRATEGIES FOR SRM DRIVE

During driving mode, the standstill battery balance and unequal SoC basing on the split convertercontrol strategyis explained in this section.

A. Split converter Control Strategy during Drive

The balance of the phase voltage is determined by $\pm U_{ab} = Ri + L(\theta)\frac{di}{dt} + iw\frac{dL(\theta)}{d\theta}$ (1)

Where;

U_{ab} = voltage of the phase
R = resistance of the phase
L =inductance of the phase
i = current of the phase
θ=Angular position of the rotor
ω = Angular velocity.

WhenU_{ab} isa positive voltage (+),it can be in excitation and the battery discharges. If it is a negative voltage ($-U_{ab}$), works in the demagnetization or regenerative braking mode and the battery is charged. Basing on the position of the rotor the inductance of the phase varies and the torque given as,

$$T_e = \frac{1}{2} i^2 \frac{dL(\theta)}{d\theta} \quad (2)$$

whereT_e= Electromagnetic torque of the phase
A positive torque(T_e>0) and negative torque (T_e<0) is generated when the inductance of phase winding are excited by current i.e; ($dL/d\theta$>0) and ($dL/d\theta$<0). Hence controlling of electromagnetic torque is attained by changingthe turn-on angle (θ_{on}) and turn-off-angle (θ_{off}).
The SRM's mechanical motion equation is provided by

$$J\frac{dW}{dt} + B\omega = \sum T_{ek} - T_l \quad (3)$$

Where;

J = combined moment of motor and load inertia
B = combined motor and load friction coefficient
T_{ek}= combined electromagnetic torque
T_l= load torque

The demagnetized mode of SRM control block diagram is displayed in Fig. 2. The four-phase power converter is split into two converters (A and B act as one phase and C and D act as one). From fig 1 U_{ab}as E1 is applied to converter I andU_{cd}asE2 applied to converter II. The braking torque can be generated during regenerative braking mode by converter I or converter II and recover the braking energy.In the driving mode, this converter can achieve SoC battery balance. Here the closed loop speed control operation depends on the rotor angular position. Moreover, the operational modes depend on the gating pulses of the converter switches. During motoring mode, the positive torque is produced where the speed reference is more than the actual speed by the active inductances of windings and alsothe battery is in a dischargedstate. Otherwise, in regenerative braking mode, it produces a negative torque and battery is charged. Because of the split phase in SRM, it has good fault tolerance capability. If phases are defective (e.g., C–D), the engine can nevertheless operate while the currents are increased in healthy phases (A–B).

B. Battery Balancing in the stand Still Scenario

Due to the different voltages concerning the batteries and phase windings, SoC levels are different for batteries. In the standstill scenario in order to balance the U_{ab} and U_{cd} voltages between phases, node NA is connected to ND as presented in Fig. 3(a). Fig 3(b) and (c) display the phase

excitation and charging status, respectively. In the picture. 3(b), S0 and S3 perform winding inductance charges. Fig.3(c) shows the discharging state of excited inductive winding to the E2 battery. When the E1 battery SoC is lower than that of the E2, S1, S5, and S6 battery, the winding inductance charging is switched on. Battery E1 is charged by switching off devices S1 and S6.

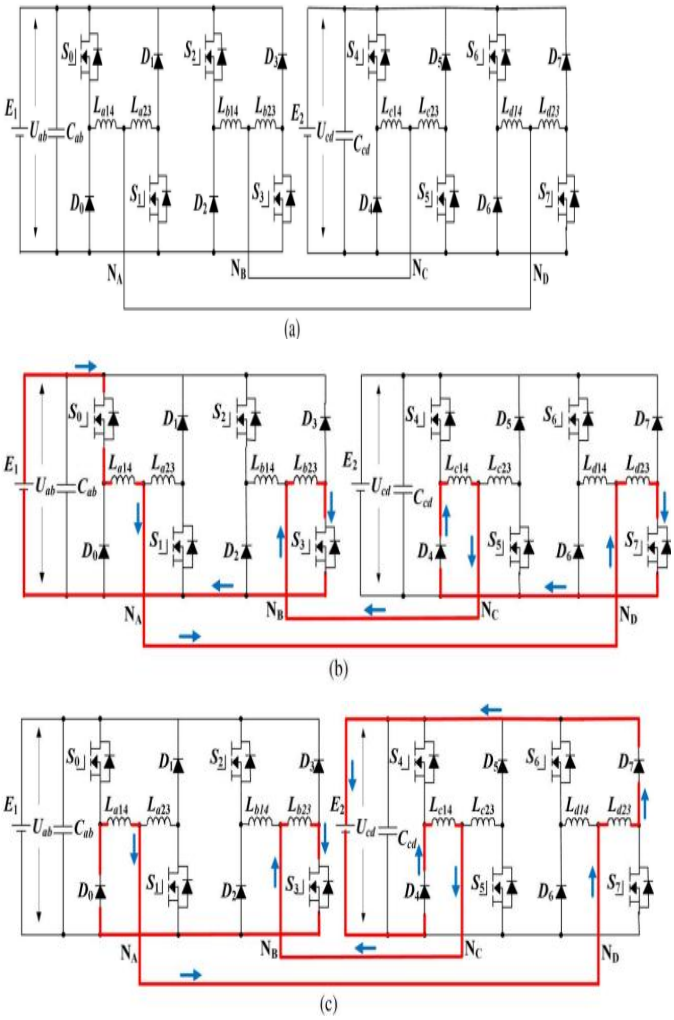

Fig. 3. Balance of battery voltage in working conditions. (A) Battery voltage equalization. (B) Phase winding excitation status. (C) E2 charging status.

C. Unequal SoC in a mode of driving

During driving mode, the two batteries are having different SoC levels as a result of the fluctuating motor parameters and battery characteristics.The average phase voltage for phases A and C is expressed in the excitation region.

$$U_a = DU_{ab} = R_a i + L_a(\theta)\frac{di_a}{dt} + i_a\omega\frac{dL_a(\theta)}{d\theta} \quad (4)$$

$$U_c = DU_{cd} = R_c i + L_c(\theta)\frac{di_c}{dt} + i_c\omega\frac{dL_c(\theta)}{d\theta} \quad (5)$$

Where
U_a and U_c= phase-A and phase-C voltages
D =duty cycle for the modulation of the voltage pulse width.

The imbalance between phase A and C i.e. phase A average voltage is greater than phase C, due to the sharing of same PWM duty cycle by converter I and II.

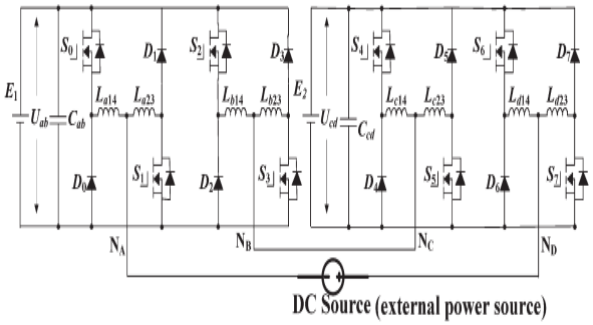

Fig.4. DC power charging of batteries.

Nevertheless, due to the closed-loop control operation, the system can still operate steadily. The four-phase currents are balanced by using the current regulatory control, even though the input voltages for converters I and II are different.

IV. CHARGING MODE OFCONTROL

The dc and ac charging is supported by the proposed dual-split converter.

A.DC Charging

From Fig. 4. The proposed converter acts as a boost converter where the Two converters (U_{ab} and U_{cd}). Voltageresponse is greater than the applied DC source voltage. This Low-voltage dc power (e.g. from a dc micro grid) can charge the batteries Usually;on-board battery voltage istwice than the DC source voltage available in an EV/HEV structure. As illustrated in Fig.5, there are four basic working states. In state 1 operation, Only S3 and S7 conduct. During this operation, the DCcharges the winding inductances L_{a14}, L_{b23}, L_{c14} and L_{d23};hence,it is possible to express the corresponding voltage equation.

$$U_{dc} = (L_{a14} + L_{b23} + L_{c14} + L_{d23})\frac{di_s}{dt} \quad (6)$$

Where U_{dc}= output voltage

i_s= output current

All MOSFETs stop conducting in stage 2 of work. The dc source and winding inductances (La14, Lb23, Lc14, and Ld23) simultaneously discharge the energy into both batteries, i.e.

$$U_{dc} = (L_{a14} + L_{b23} + L_{c14} + L_{d23})\frac{di_s}{dt} + U_{ab} + U_{cd} \quad (7)$$

S3 conducts at work stage 3. The dc source and winding inductances (La14, Lb23, Lc14, and Ld23) release the energy into the E2 battery, i.e.

$$U_{dc} = (L_{a14} + L_{b23} + L_{c14} + L_{d23})\frac{di_s}{dt} + U_{cd} \quad (8)$$

S7 conducts at work stage 4. The dc source and winding inductances (La14, Lb23, Lc14, and Ld23) release the energy into the E1 battery, i.e.

$$U_{dc} = (L_{a14} + L_{b23} + L_{c14} + L_{d23})\frac{di_s}{dt} + U_{ab} \quad (9)$$

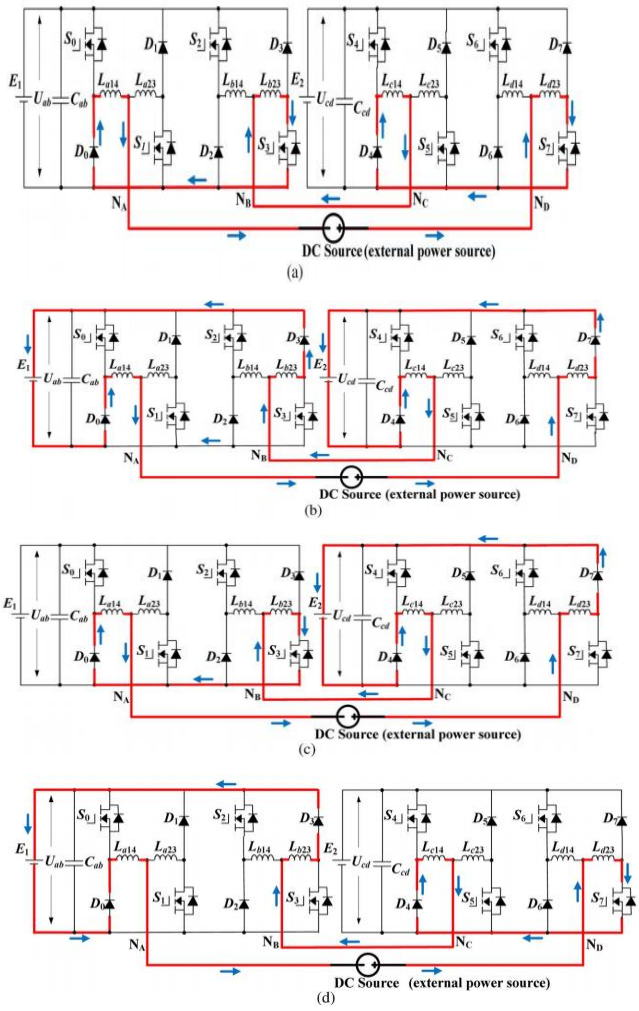

Fig.5. Low voltage external power source Operational states. (a) State 1. (b) State 2. (c) State 3. (d) State 4.

B. AC Charging

As shown in Fig 6(a), a single phase AC source is connected as an external power source to charge the batteries. This is a typical multilevel cascading topology. There are five levels of output voltage: 0, U_{ab}, $U_{ab}+U_{cd}$, $-U_{ab}$, and $-(U_{ab}+U_{cd})$. In turn, to reduce the switching frequency and enhance power quality, the multi-stage hysteresis control is used in charging control, as shown in Fig 6(b). Let SoCI and SoCIIare the E1 battery SoC and the E2 battery SoC respectively. The SoC influence is considered in the proposed control strategy. The energy charged to the E1 and E2 batteries is the same when the two batteries have the same SoC. In Fig. 7 Presents the voltage output over a frequency cycle of one line. It is observed that switching frequency and total harmonic distortion (THD) is decreased in a half cycle by five output voltage stages. The charging voltages of E1 and E2 battery are identical due to the symmetry of the switching actions.

Table.1 lists the corresponding switching device actions.

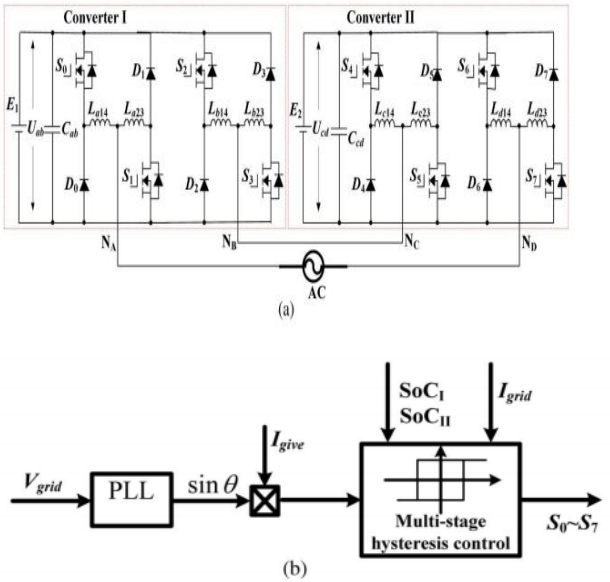

Fig. 6 Operation of a converter by Alternating Current charging and its control (a) Batteries charging by AC power (b) Multi-stage control of hysteresis

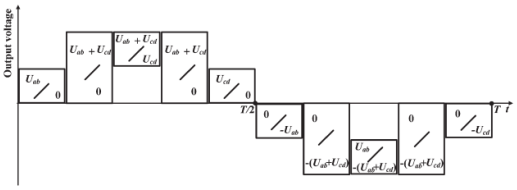

Fig. 7. DZUnder multi-stage hysteresis control (SoCI= SoCII), output voltage levels.

Table 1
Switching operation by multi-stage hysteresis controller (positive half-cycle)

Stage	Low voltage level		High voltage level	
	Output voltage	Conducting devices	Output voltage	Conducting devices
1	0	S_1,S_3,S_5,S_7	U_{ab}	D_1,S_3,S_5,S_7
2	0	S_1,S_3,S_5,S_7	$U_{ab}+U_{cd}$	D_1,S_3,S_5,S_7
3	U_{cd}	S_1,S_3,S_5,S_7	$U_{ab}+U_{cd}$	D_1,S_3,S_5,S_7
4	0	S_1,S_3,S_5,S_7	$U_{ab}+U_{cd}$	D_1,S_3,S_5,S_7
5	0	S_1,S_3,S_5,S_7	U_{cd}	S_1,S_3,S_5,S_7

TABLE 2
Unequal strategies for charging SoCs (positive half-cycle)

Stage	$SoC_I > SoC_{II}$		$SoC_I < SoC_{II}$	
	High voltage level	Low voltage level	High voltage level	Low voltage level
1	U_{cd}	0	U_{ab}	0
2	$U_{ab}+U_{cd}$	0	$U_{ab}+U_{cd}$	0

3	$U_{ab}+U_{cd}$	U_{cd}	$U_{ab}+U_{cd}$	U_{ab}
4	$U_{ab}+U_{cd}$	0	$U_{ab}+U_{cd}$	0
5	U_{cd}	0	U_{ab}	0

The frequency of switching for the three stages is set by

$$f_{1,5} = \frac{U_{grid}\ (U_{ab}-U_{grid})}{HL_{ABCD}U_{ab}} \quad (10)$$

$$f_{2,4} = \frac{U_{grid}\ (U_{ab}+U_{cd}-U_{grid})}{HL_{ABCD}(U_{ab}+U_{cd})} (11)$$

$$f_{3} = \frac{(U_{grid}\ -U_{ab})(U_{ab}+U_{cd}-U_{grid})}{HL_{ABCD}U_{cd}} (12)$$

Whereas,
$f_{1,5}$= switching frequency for stages 1 and 5
$f_{2,4}$= switching frequency for stages2 and 4
f_3= switching frequency for stage 3
U_{grid} = instant grid voltage
H = hysteresis control bandwidth
L_{ABCD}= inductance of the circuit, which is the sum of half inductance (e.g., L_{a14}) of phases A, B, C, and D.
The unequal charging strategy for SoC is presented in Table.2. When $SoCU_{ab}<SoCU_{cd}$, more energy is charged to the E1 battery than to the II battery. In stages 1–5, the grid charges the battery E1, while the stages 2–4 charges the battery E2. If SoCI > SoCII charges the E1 battery less than the E2 battery. In stages 1–5, the grid charges the battery E2 while the stages 2–4 charges the battery E1.

C. Influence of different phase inductivities

The circuit inductance is required for the design of the control loop insources, DC and AC charging conditions. Because of the doubly salient SRM, the inductances of the phase always vary with the position of the rotor. Luckily, the sum of the four inductances over the rotor position becomes much more stable than the phase inductances. It is therefore used for designing control loops.

V. HYBRID FUZZY CONTROLLER

The main objective of the hybrid controller's (combination of PI and fuzzy logic controllers) is to obtain better response than an individual controller. Two major differences exist between the conventional PI controller's tracking ability and the fuzzy logic controller. In steady state,both the PI and the fuzzy controller produce moderately good tracking. Nevertheless, a small variation in operation will exhibit some oscillation in the PI controller due to its fast response, impact on load. However, under same operating condition fuzzy controller reduces oscillations even it has a slower response. Hence a combination of controllers gives quick response and eliminates associated oscillations in the system.To justify individual performance switching control strategy is required. If it requires the advantage of PI controller fast response, use it for a long time, andit is necessary to observe that fuzzy controller usage is only the system under oscillation. Therefore it is necessary to exploit a methodof switching from PI to the fuzzy controller;it can be possible by basing on two conditions.

1) Switch on detection of oscillations; 2) Switch on detection of overshoot. In the Fuzzy Logic controller basing on *IF-THEN*rules the switching process takes place. *IF* the system is activated with an oscillatory behaviour*THEN* fuzzy controller, the PI controller will be operated otherwise. When the error is zero, the system processed is considered to have overshot, and the rate of error alters is any value other than zero. To measure the system, oscillations the measured and absolute values under the same period has to be considered. Since the system is predictable to overshoot during oscillatory behaviour, the only condition to be considered for switching is overshooting. In practiceNevertheless, it is more useful to implement the control signal directly by the controller's control actions. The fuzzy controller can, therefore, be designed in such a way that normal behaviour (no oscillations or over-shooting) leads to a null-fuzzy action. Consequently, when the fuzzy has a null value, the switch between the two controllers diminishes the use of PI; otherwise, the fuzzy output is used.

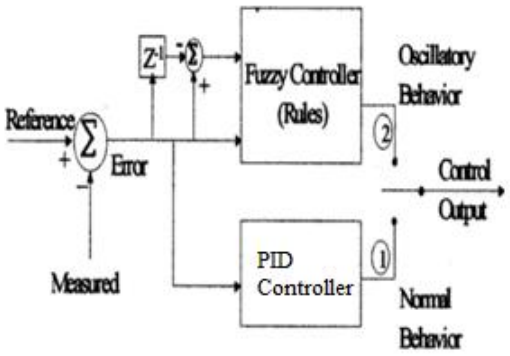

Fig.8. Switching mechanism structure in a null-fuzzy action.

VI. MATLAB/SIMULATION RESULTS

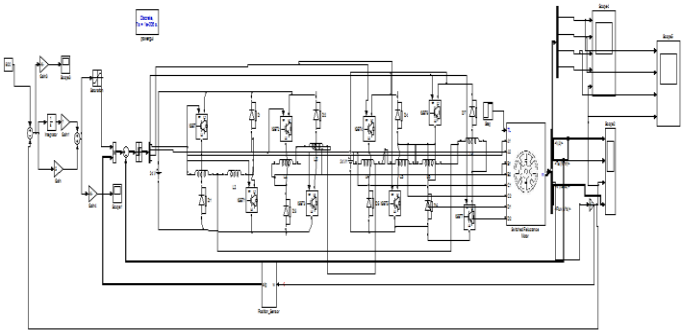

Fig.9.Matlab / Simulation Model Battery voltage equalization with PI

Controller.

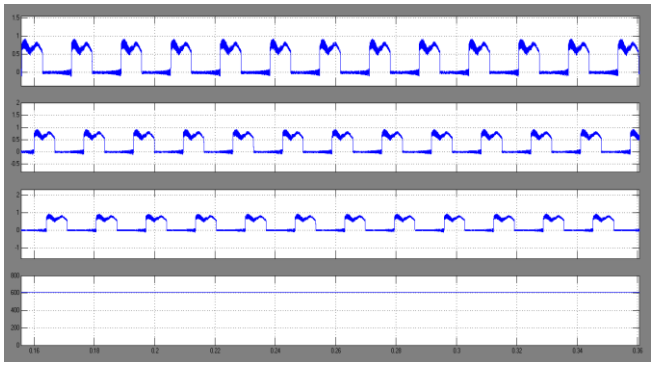

Fig. 10. Simulation results of $_{IA}$, I_b, $I_c$and Speed driving mode.

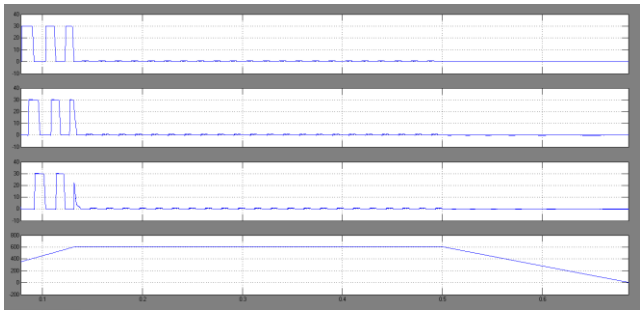

Fig. 11. Simulation results of I_a, I_b, I_c and speed driving mode with Braking under normal condition.

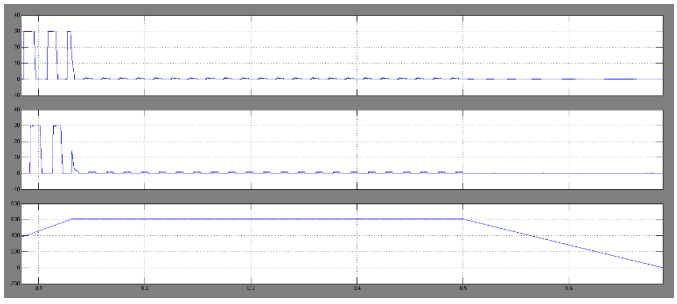

Fig. 12. Simulation results in the driving mode of the phase currents (I_b, I_c) and speed batteries with Braking under unequal SoC.

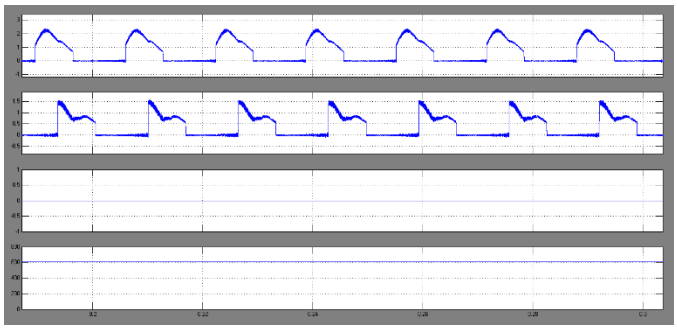

Fig. 13. Simulation results in driving mode with Phase Currents (I_a,I_b,I_c) and Speed Fault-tolerant operation

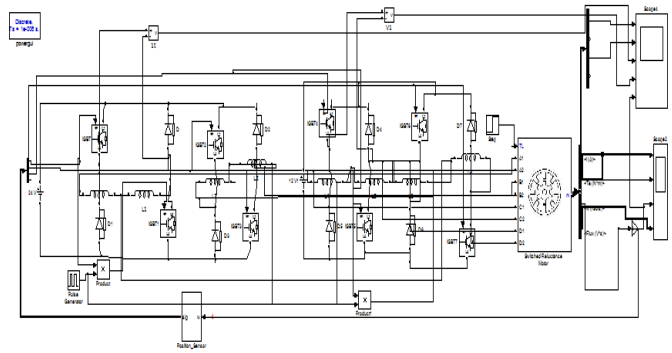

Fig.14.Model Matlab / Simulation of the different voltages of the battery

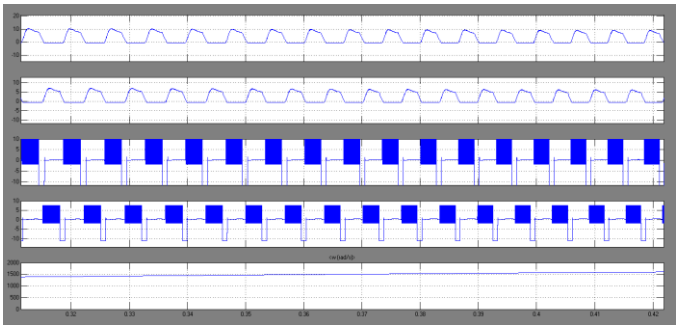

Fig. 15 Response of unequal and equal voltage sources at Pulse controllers of switches(a) 12 V PWM (E1)−9.6 V.

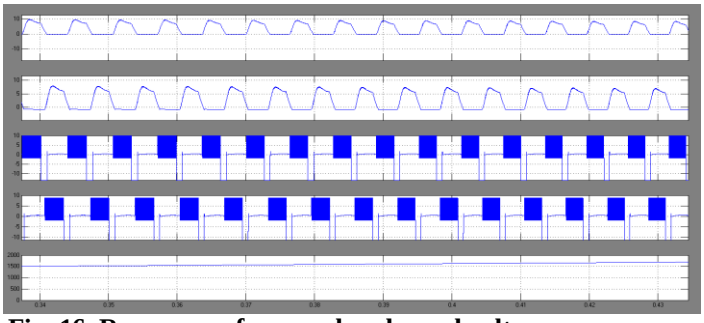

Fig. 16. Responses of unequal and equal voltage sources, at Pulse controllers of switches (a) 12V(E_1)−10.8 V(E_2) PWM.

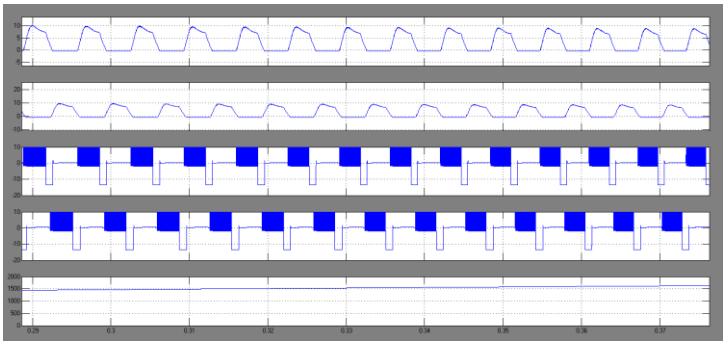

Fig. 17. Responses of unequal and equal voltage sources, at Pulse controllers of switches (a) 12V(E_1) −12 V(E_2) PWM

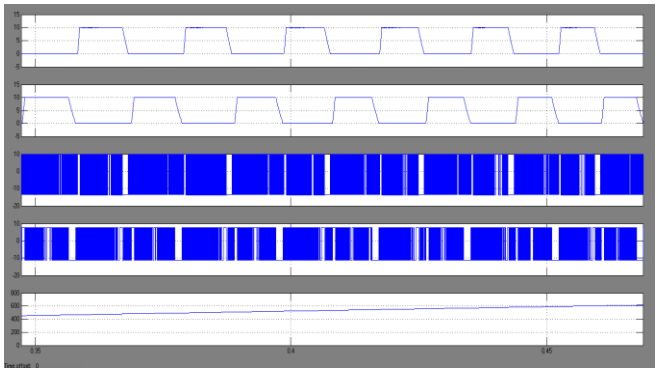

Fig. 18Pulse controllers of switches with equalandunequalvoltage sources (a) 12 V PWM (E_1)−9.6 V(E_2).

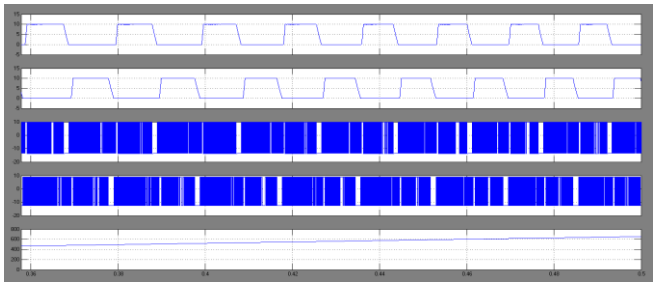

Fig. 19. Pulse controllers of switches with equalandunequalvoltage sources(a) 12 V PWM (E_1)−10.8 V(E_2).

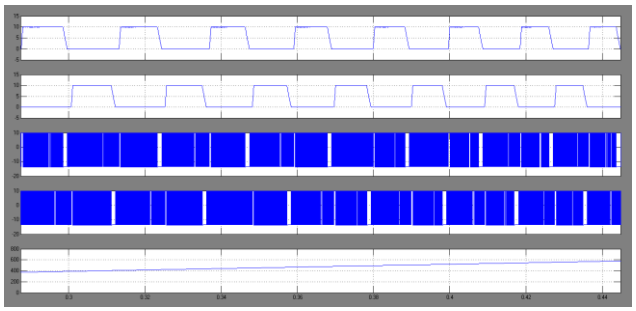

Fig. 20. PWM and current chopping control (CCC) with equalandunequalvoltage sources. (a) 12 V PWM (E1)−.12 V(E2).

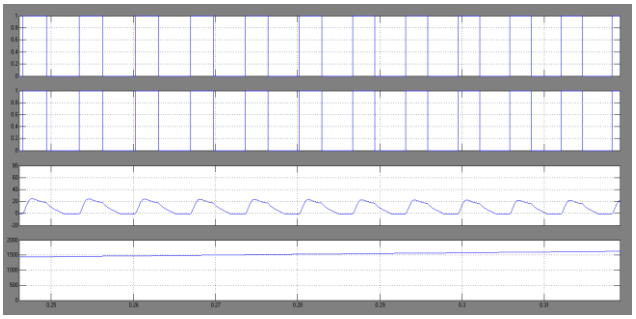

Fig.21.simulation responses of switches(S0 and S7),current (I_{ad}) and speed ofbattery voltage

equalization.

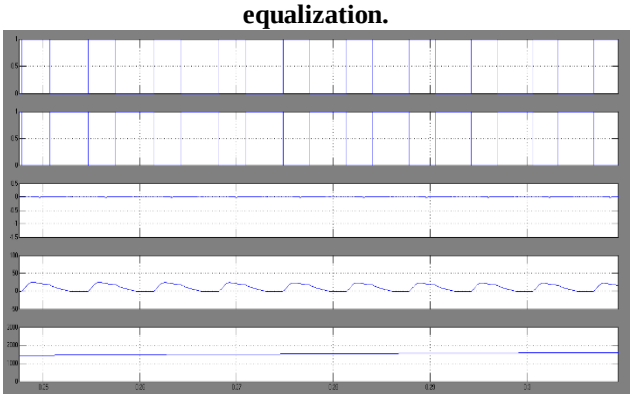

Fig.22.Simulation Responses of switches (S3 and S7), Current (I_s) and speed of DC charging.

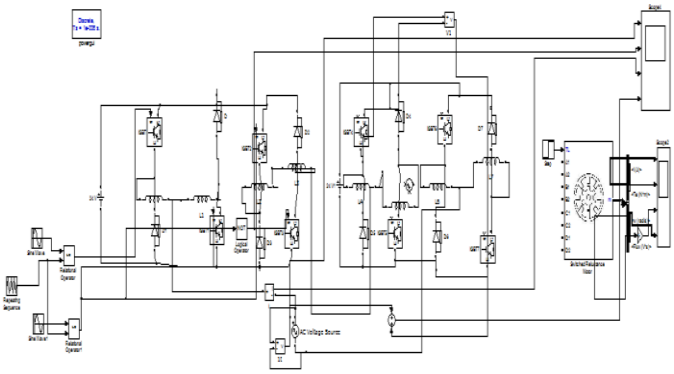

Fig.23.Simulink model with AC source under charging mode

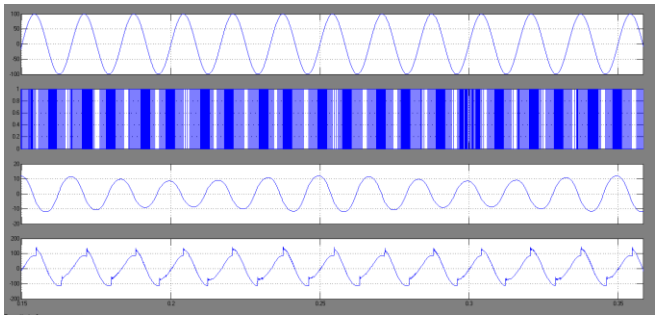

Fig.24.Grid voltage, switch voltage, Current and Voltage (Ucd) grid simulation waveform.

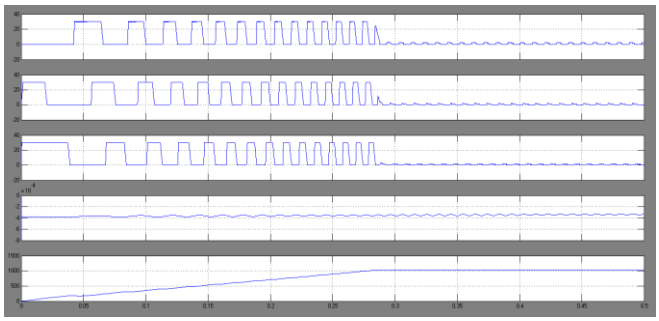

Fig.25.Simulation results in Braking driving mode under normal phase currents conditions (Ia, Ib, Ic) and PI Controller speed.

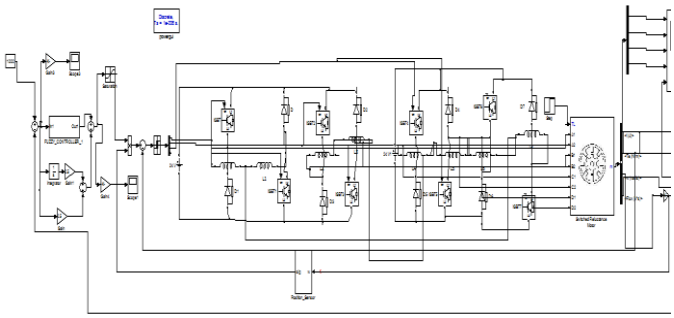

Fig.26.Matlab / Simulation Model Battery voltage equalization with Hybrid Fuzzy Logic Controller.

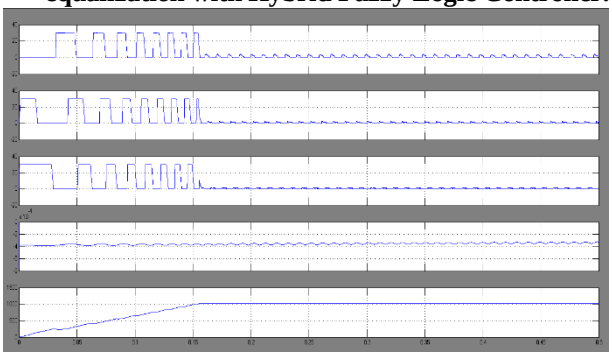

Fig.27.Simulation results in phase currents (I_a,I_b,I_c) and hybrid fuzzy logic controller driving mode with Braking under normal condition.

VII. CONCLUSION

An8pole SRM is analyzed with both AC and DC external sources in terms of torque capacity, torque ripple, average speed, and speed ripple, the electromagnetic performance. The basicsingle-phase full bridge converter is used to produce unidirectional current flow in SRM phases. In order to reduce the weight of the converter and cost-effectiveDC link is removed. In DC excitation, lower torque and speed are observed. Due to lower current harmonics at high current reference, the iron loss with sinusoidal excitation is significantly reduced. Thus the efficiency at high speed will be high. The speed control of the SRM motor by hybrid Fuzzy Logic Controller is compared with conventional methods of Proportional and Proportional Integral. Hence concluded that the Hybrid Fuzzy Logic Controller provides the required output compared to the other controllers. The hybrid fuzzy logic controller ensures excellent reference tracking of switched reluctancemotor drives in this proposed method. This hybrid fuzzy logic controller gives without overshooting the best speed tracking and enhances speed regulation.

REFERENCES

1. M. R. Mohamed, P. K. Leung, and M. H. Sulaiman, "Performance characterization of a vanadium redox flow battery at different operating parameters under a standardized test-bed system," Applied Energy, vol. 137, pp. 402-412, Jan 2015, doi: 10.1016/j.apenergy.2014.10.042.
2. B. K. Bose, "Global Energy Scenario and Impact of Power Electronics in 21st Century," Ieee Transactions on Industrial Electronics, vol. 60, no. 7, pp. 2638-2651, Jul 2013, doi: 10.1109/tie.2012.2203771.
3. J. de Santiago et al., "Electrical Motor Drivelines in Commercial All-Electric Vehicles: A Review," (in English), Ieee Transactions on Vehicular Technology, vol. 61, no. 2, pp. 475-484, Feb 2012, doi: 10.1109/Tvt.2011.2177873.
4. A. Chiba, K. Kiyota, N. Hoshi, M. Takemoto, and S. Ogasawara, "Development of a Rare-Earth-Free SR Motor With High Torque Density for Hybrid Vehicles," Ieee Transactions on Energy Conversion, vol. 30, no. 1, pp. 175-182, Mar 2015, doi: 10.1109/tec.2014.2343962.
5. K. Kiyota, T. Kakishima, and A. Chiba, "Comparison of Test Result and Design Stage Prediction of Switched Reluctance Motor Competitive With 60-kW Rare-Earth PM Motor," Ieee Transactions on Industrial Electronics, vol. 61, no. 10, pp. 5712-5721, Oct 2014, doi: 10.1109/tie.2014.2304705.
6. S. E. Schulz, K. M. Rahman, Ieee, and I. Ieee, "High performance digital PI current regulator for EV switched reluctance motor drives," Conference Record of the 2002 Ieee Industry Applications Conference, Vols 1-4, pp. 1617-1624, 2002 2002.
7. Z. Zhu, X. Liu, and Z. J. I. T. o. E. C. Pan, "Analytical model for predicting maximum reduction levels of vibration and noise in switched reluctance machine by active vibration cancellation," vol. 26, no. 1, pp. 36-45, 2011.
8. H. Chen and S. Lu, "Fault Diagnosis Digital Method for Power Transistors in Power Converters of Switched Reluctance Motors," Ieee Transactions on Industrial Electronics, vol. 60, no. 2, pp. 749-763, Feb 2013, doi: 10.1109/tie.2012.2207661.
9. T. Ishikawa, Y. Hashimoto, and N. Kurita, "Optimum Design of a Switched Reluctance Motor Fed by Asymmetric Bridge Converter Using Experimental Design Method," Ieee Transactions on Magnetics, vol. 50, no. 2, Feb 2014, Art no. 7019304, doi: 10.1109/tmag.2013.2285584.
10. Y. Zou, K.-W. E. Cheng, N. C. Cheung, and J. Pan, "Deformation and Noise Mitigation for the Linear Switched Reluctance Motor With Skewed Teeth Structure," Ieee Transactions on Magnetics, vol. 50, no. 11, Nov 2014, Art no. 8102304, doi: 10.1109/tmag.2014.2323420.
11. R. B. Inderka and R. De Doncker, "High-dynamic direct average torque control for switched reluctance drives," Ieee Transactions on Industry Applications, vol. 39, no. 4, pp. 1040-1045, Jul-Aug 2003, doi: 10.1109/tia.2003.814579.
12. P. O. Rasmussen, J. H. Andreasen, and J. M. Pijanowski, "Structural stator spacers - A solution for noise reduction of switched reluctance motors," Ieee Transactions on Industry Applications, vol. 40, no. 2, pp. 574-581, Mar-Apr 2004, doi: 10.1109/tla.2004.824489.
13. Y. Hu, X. Song, W. Cao, and B. Ji, "New SR Drive With Integrated Charging Capacity for Plug-In Hybrid Electric Vehicles (PHEVs)," Ieee Transactions on Industrial Electronics, vol. 61, no. 10, pp. 5722-5731, Oct 2014, doi: 10.1109/tie.2014.2304699.
14. M. Budhia, J. T. Boys, G. A. Covic, and C.-Y. Huang, "Development of a Single-Sided Flux Magnetic Coupler for Electric Vehicle IPT Charging Systems," Ieee Transactions on Industrial Electronics, vol. 60, no. 1, pp. 318-328, Jan 2013, doi: 10.1109/tie.2011.2179274.